Synthesis, in vitro and in vivo studies, and molecular modeling of N-alkylated dextromethorphan derivatives as non-competitive inhibitors of α₃β₄ nicotinic acetylcholine receptor

Krzysztof Jozwiak [a,†], Katarzyna M. Targowska-Duda [a,†], Agnieszka A. Kaczor [b,c,†], Joanna Kozak [a,d], Agnieszka Ligeza [b], Elzbieta Szacon [b], Tomasz M. Wrobel [b], Barbara Budzynska [e], Grazyna Biala [e], Emilia Fornal [f], Antti Poso [c], Irving W. Wainer [g], Dariusz Matosiuk [b,*]

[a] Department of Chemistry, Laboratory of Medicinal Chemistry and Neuroengineering, Medical University of Lublin, 4a Chodzki St., PL-20093 Lublin, Poland
[b] Department of Synthesis and Chemical Technology of Pharmaceutical Substances with Computer Modeling Lab, Faculty of Pharmacy with Division of Medical Analytics, 4a Chodzki St., PL-20093 Lublin, Poland
[c] School of Pharmacy, University of Eastern Finland, Yliopistonranta 1, PO Box 1627, FI-70211 Kuopio, Finland
[d] Department of Anatomy, Medical University of Lublin, 4 Jaczewskiego St., PL-20090 Lublin, Poland
[e] Department of Pharmacology and Pharmacodynamics, Medical University of Lublin, 4a Chodzki St., PL-20093 Lublin, Poland
[f] Department of Chemistry, Catholic University of Lublin, al. Krasnicka 102, PL-20718 Lublin, Poland
[g] Laboratory of Clinical Investigation, Division of Intramural Research Programs, National Institute on Aging, National Institutes of Health, Baltimore, MD 21224, USA

ARTICLE INFO

ABSTRACT

9 N-alkylated derivatives of dextromethorphan are synthesized and studied as non-competitive inhibitors of α3β4 nicotinic acetylcholine receptors (nAChRs). In vitro activity towards α3β4 nicotinic acetylcholine receptor is determined using a patch-clamp technique and is in the micromolar range. Homology modeling, molecular docking and molecular dynamics of ligand-receptor complexes in POPC membrane are used to find the mode of interactions of N-alkylated dextromethorphan derivatives with α3β4 nAChR. The compounds, similarly as dextromethorphan, interact with the middle portion of α3β4 nAChR ion channel. Finally, behavioral tests confirmed potential application of the studied compounds for the treatment of addiction.

© 2014 Elsevier Ltd. All rights reserved.

1. Introduction

Nicotinic acetylcholine receptors (nAChRs) are members of the ligand gated ion channel family[1] and they are distributed at the synaptic junctions of brain neurons where they regulate the release of several neurotransmitters. Furthermore they are abundant in the periphery where they mediate synaptic transmission at the neuromuscular junction and ganglia.[2] In this regard, nAChRs are involved in several physiologically relevant functions such as cognition, memory, pain perception, auditory response, muscle contraction, angiogenesis, and immune response.[1]

nAChRs are members of the Cys-loop ligand-gated ion channel superfamily and consists of five separate transmembrane proteins (subunits), each containing a large extracellular N-terminal domain, four membrane-spanning helices (M1, M2, M3, and M4), and a small C-terminal domain.[1,3]

In addition to the binding site of endogenous neurotransmitter and other orthosteric ligands, the receptor contains several allosteric binding sites at which noncompetitive inhibitors (NCIs) may bind.[4–6] The most important binding site for NCIs is the luminal high-affinity domain, which is located on the internal surface of the ion pore lined predominantly with five M2 helices, each incorporated by separate subunit.

Several subtypes of nAChR pose attractive possibility as drug targets, one of them, α3β4 subtype known to be expressed in ventral tegmental area, medial habenula, interpeduncular nucleus, pineal gland, locus coeruleus, dorsolateral tegmentum, basolateral amygdale, and hippocampus[7,8] has been particularly studied as a target for drug addiction. For example, Toll et al., has recently reported a novel high affinity and highly selective α3β4 nAChR antagonist with potent blocking activity of nicotine self-administration in rats.[9] It has been postulated that α3β4 nAChRs inhibitory activity is related to the anti-addictive properties.[10]

* Corresponding author. Tel./fax: +48 81448 7272.
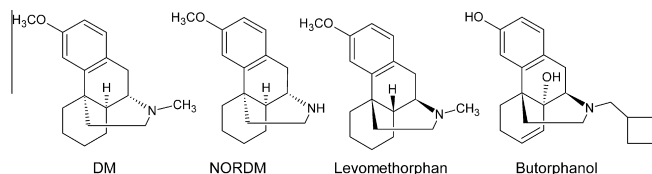 E-mail address: darek.matosiuk@umlub.pl (D. Matosiuk).
† Equal contributors.

Figure 1. Morphinan's derivatives as NCIs of α3β4 nAChR.

Additional studies support the view that β4-containing nAChRs (i.e., α3β4, α3β3β4) play a major role in the appearance of nicotine withdrawal symptoms as well as in mediating the negative-reinforcing properties.[11,12] Moreover, there is some evidence that α3β4 nAChRs are involved in the expression of at least two signs of opioid withdrawal.[13]

Dextromethorphan (DM) (Fig. 1) and its metabolite dextrorphan have been identified to reduce morphine, methamphetamine and nicotine self-administration in rats.[14] These compounds are primarily known to inhibit NMDA glutamate receptors,[15] our previous studies, however, have determined them, along with other morphinan analogs (Fig. 1), as potent NCIs of the α3β4 nAChR.[6,16,17] In affinity chromatography assay DM molecule has shown high affinity to the luminal binding site of the α3β4 nAChR receptor immobilized on the stationary phase. Intriguingly, the opposite enantiomer, levomethorphan has its affinity significantly reduced in comparison to DM. Non-linear chromatography model has identified dissociation kinetics of the drug–receptor complex as responsible for observed affinity difference of the two enantiomers to the receptor.[18] Subsequent molecular modeling study has postulated that the difference lies in the differential orientation of the two isomeric molecules within the lipophilic cleft formed in the channel lumen.[6] As result, the amino moiety of DM molecule is located in optimized position to form a hydrogen bond with neighboring serine residues while corresponding moiety of levomethorphan lies in further distance preventing such an interaction. Interestingly, due to single point polymorphism present in the M2 helix of β subunits, the specific cleft binding morphinan analogs occurs only in nAChRs containing β4 component but not in β2 containing subtypes.[6] The finding has lead us to initiate rational design of new DM derivatives which while modified at the amino alkyl moiety seems to be additionally optimized for selective interactions with the nAChR subtypes containing β4 subunits and in particular with natural target for addiction, α3β4 nAChR.

Current work presents synthesis of novel N-alkylated DM derivatives, and their investigations as NCIs of the α3β4 nAChR. The pharmacological activity of the studied compounds determined using a patch-clamp technique was in the micromolar range. Furthermore, we applied homology modeling, molecular docking and molecular dynamics to demonstrate ligand–receptor interactions involving nicotinic receptor ion channel domain. Finally, in the light of our behavioral studies the novel derivatives have potential application for the treatment of drug addiction.

2. Materials and methods

2.1. Chemistry

NMR spectra were acquired using Bruker Avance 400 spectrometer. MS spectra with nanospectrospray ionization (nano ESI) were recorded with Agilent Technologies 6538 UHD Accurate Mas Q-TOF LC/MS mass spectrometer on the nano-LC-chip-QTOF system. The elementary analysis was performed with the application of Perkin–Elmer analyzer. Melting points were determined with Boetius apparatus.

2.1.1. Demethylation of DM

A solution of 2.68 g (67 mmol) of sodium hydroxide in 50 ml of water was added to a solution of 25 g (67 mmol) of dextromethorphan hydrobromide hydrate in 100 ml of chloroform. The reaction mixture was stirred for 30 min on a magnetic stirrer. The organic layer was separated and dried with anhydrous sodium sulfate. The solvent was evaporated on a rotavap. The obtained freebase of dextromethorphan was a dense and viscous off-white oil which solidified upon standing. Yield: 17.95 g (97.98%). Dextromethorphan freebase (17.95 g, 63 mmol), 250 ml of toluene and 15.28 g (72.1 mmol) of 2,2,2-trichloroethyl chloroformate was heated under gentle reflux for 2 h. The reaction mixture was washed with 50 ml of 5% hydrochloric acid and 50 ml of water. The organic layer was separated and dried with anhydrous sodium sulfate. Toluene was removed on a rotatory evaporator under reduced pressure. The crude product was purified by flash chromatography on silica gel using hexane/ethyl acetate as a mobile phase. Thus there was obtained 25.54 g (91.2%) of white solid. The obtained 2,2,2-trichloroethyl (9α,13α,14α)-3-methoxymorphinan-17-carboxylate (25.54 g, 57.2 mmol) and 250 ml of 90% acetic acid was stirred on a magnetic stirrer and 11.22 g (171.6 mmol) of zinc powder was added in portions during 30 min. After 1 h of additional mixing the remaining zinc was filtered and acetic acid was evaporated on a rotatory evaporator under reduced pressure. 50 ml of toluene was added to the obtained dense oil, this was brought to boiling and the mixture was allowed to cool down in a refrigerator. The resulting white precipitate of (9α,13α,14α)-3-methoxymorphinan tetraacetozincate was filtered and washed with diethyl ether, yield: 34.84 g (72%). The obtained (9α,13α,14α)-3-methoxymorphinan tetraacetozincate (34.84 g, 41.2 mmol–82.4 mmol equiv) was dissolved in 50 ml of chloroform and 75 ml of 1 M sodium hydroxide solution was added. The white precipitate was filtered, washed with chloroform and organic layer separated. The aqueous layer was extracted 4 times with 25 ml of chloroform and chloroform layers were combined and dried with anhydrous sodium sulfate. The solution was stripped of solvent to afford clear oil of (9α,13α,14α)-3-methoxymorphinan (nordextromethorphan) which solidified upon standing. Yield: 12.47 g (55.81%).

2.1.2. Synthesis of N-alkylated derivatives of DM (compounds 1–9), method A

1.08 g (4 mmol) of (9α,13α,14α)-3-methoxymorphinan, 5 mmol of bromo- or chloroalkylating agent, 2 g of triethylamine and 20 ml of anhydrous ethanol or acetonitrile was heated under nitrogen atmosphere in mild boiling of the solvent for 2–24 h. The solvent was evaporated under reduced pressure and 20 ml of 20% solution of sodium carbonate was added to the resulted oil. The obtained mixture was extracted 4 times with 25 ml of chloroform. The organic layers were dried with anhydrous sodium sulphate. The obtained precipitate of hydrobromide or hydrochloride was washed with diethyl ether. Reactions were routinely monitored with thin-layer chromatography (TLC) on silica gel (60 F$_{254}$ Merck plates) in two eluent systems: 80% acetic acid–chloroform–methanol (1:8:1) (A) and 5% NH$_4$OH in MeOH–dioxane (5:95) (B) and the products were visualized with ultraviolet light of 254 nm wavelength.

2.1.2.1. (9α,13α,14α)-17-Cyanomethyl-3-methoxymorphinan hydrobromide, 1, C$_{19}$H$_{25}$BrN$_2$O. The reaction mixture was heated for 11 h and the white crystalline precipitate of **1** was obtained. Yield: 1.31 g (86.60%). Mp 206–207 °C, R_f: 0.727 (A) and 0.663 (B). ^{1}H NMR (d_6-DMSO): 8.81 (s, 1H); 7.10–7.12 (m, 1H); 6.81–6.84 (m, 2H); 4.73 (s, 2H); 3.73 (s, 3H) 3.54 (s, 1H); 3.19–3.21 (m, 1H); 3.14 (s, 1H); 3.02–3.08 (m, 1H); 2.60 (s, 1H); 2.43–2.47 (m, 1H); 2.08–2.11 (m, 1H); 1.90 (s, 1H); 1.59–1.62 (m, 1H); 1.45–1.52 (m, 3H); 1.29–1.33 (m, 2H); 1.07–1.17 (m, 1H);

0.9–1.00 (m, 1H); ^{13}C NMR (d_6-DMSO): 158.12, 141.80, 130.25, 128.31, 117.09, 115.59, 110.77, 59.36, 55.29, 46.78, 46.54, 38.46, 38.35, 37.79, 37.17, 24.75, 23.91, 20.19. MS: calcd for $C_{19}H_{24}N_2O$ 296.1889; found 296.1890, [M+H]$^+$ 297.1962; Anal. calcd C, 60.48; H, 6.68; N, 7.42; O, 4.24; Br, 21.18; found C, 60.51; H, 6.69; N, 7.43; O, 4.25; Br, 21.12.

2.1.2.2. (9α,13α,14α)-17-(2-Cyanoethyl])-3-methoxymorphinan hydrochloride, 2, $C_{20}H_{27}ClN_2O$. The reaction mixture was heated for 2 h and the white crystalline precipitate of **2** was obtained. Yield: 1.06 g (85.40%). Mp 223–226 °C, R_f: 0.597 (A) and 0.625 (B). ^{1}H NMR (d_6-DMSO): 11.38–11.52 (m, 1H); 7.11–7.12 (m, 1H); 6.81–6.83 (m, 2H); 3.73 (s, 3H); 3.68 (s, 1H); 3.50–3.66 (m, 2H); 3.19–3.27 (m, 2H); 3.14 (s, 2H); 2.92–2.98 (m, 1H); 2.43–2.47(m, 2H); 2.25–2.28 (m, 1H); 1.92–2.00 (m, 1H); 1.59–1.62 (m, 1H); 1.42–1.53 (m, 3H); 1.26–1.33 (m, 2H); 1.13–1.23 (m, 1H); 0.90–1.00 (m, 1H); ^{13}C NMR (d_6-DMSO): 158.52, 138.60, 129.30, 125.84, 117.79, 112.15, 110.58, 57.07, 55.04, 47.83, 40.87, 39.52, 38.27, 35.83, 34.76, 25.35, 25.31, 22.79, 21.41, 12.80, MS: calcd for $C_{20}H_{26}N_2O$ 310.4332, found 310.2048 [M+H]$^+$ 311.2121. Anal calcd C, 69.25; H, 7.85; N, 8.08; O, 4.61; Cl, 10.22; found C, 69.23; H, 7.85; N, 8.08; O, 4.61; Cl, 10.24.

2.1.2.3. (9α,13α,14α)-17-(3-Cyanopropyl)-3-methoxymorphinan hydrobromide, 3, $C_{21}H_{29}BrN_2O$. The reaction mixture was heated for 13 h and the white crystalline precipitate of **3** was obtained. Yield: 1.20 g (92.31%). Mp 230–232 °C, R_f: 0.551 (A) and 0.510 (B). ^{1}H NMR (d_6-DMSO): 9.57–9.74 (m, 1H); 7.12–7.14 (m, 1H); 6.81–6.84 (m, 2H); 3.73 (s, 4H); 3.14–3.25 (m, 3H); 3.09 (s, 1H); 2.95–3.02 (m, 1H); 2.62–2.66 (m, 2H); 2.42–2.49 (m, 2H); 2.00–2.13 (m, 3H); 1.86–1.94 (m, 1H); 1.60–1.63 (m, 1H); 1.49–1.52 (m, 3H); 1.25–1.32 (m, 2H); 1.10–1.17 (m, 1H); 0.90–0,99 (m, 1H). ^{13}C NMR (d_6-DMSO): 158.54, 138.65, 129.22, 125.78, 119.72, 112.17, 110.64, 56.91, 55.05, 51.72, 46.18, 39.52, 38.50, 35.87, 34.79, 25.37, 25.25, 22.63, 21.41, 19.92, 14.03. MS: calcd for $C_{21}H_{28}N_2O$ 324.6324; found 3245.6318, [M+H]$^+$ 325.2640. Anal calcd C, 62.22; H, 7.21; N, 6.91; O, 3.95; Br, 19.71; found C, 62.12; H 7.12; N, 6.88; O 3.91; Br 19.97.

2.1.2.4. (9α,13α,14α)-17-Amidomethyl-3-methoxmorphinan hydrobromide, 4, $C_{19}H_{27}BrN_2O_2$. The reaction mixture was heated for 15 h and the white crystalline precipitate of **4** was obtained. Yield: 0.73 g (58.10%). Mp 247–250 °C, R_f: 0.727 (A) and 0.650 (B). ^{1}H NMR (d_6-DMSO): 9.88–10.09 (m, 1H); 8.16–8.20 (m, 1H); 7.70–7.76 (m, 1H), 7.10–7.14 (m, 1H); 6.81–6.83 (m, 2H); 4.00–4.34 (m, 2H); 3.72 (s, 4H); 3.25–3.30 (m, 1H); 3.11–3.16 (m, 1H); 2.98–3.04 (m, 1H); 2.77–2.84 (m, 1H); 2.43–2.46 (m, 1H); 2.14–2.38 (m, 1H); 1.90–1.98 (m, 1H); 1.58–1.61 (m, 1H); 1.40–1.52 (m, 3H); 1.25–1.36 (m, 2H); 1.10–1.17 (m, 1H); 0.91–0.95 (m, 1H). ^{13}C NMR (d_6-DMSO): 168.72, 158.57, 138.72, 129.27, 125.73, 112.16, 110.64, 58.47, 55.07, 52.46, 46.79, 39.53, 38.37, 35.68, 34.77, 27.94, 25.03, 23.39, 21.44. MS: calcd for $C_{19}H_{26}N_2O_2$ 314.4219, found 314.1999; [M+H]$^+$ 315.2072. Anal calcd C, 57.72; H, 6.88; N, 7.09; O, 8.09; Br, 20.21; found C, 57.60; H, 6.80; N, 7.04; O, 8.05; Br, 20.51.

2.1.2.5. (9α,13α,14α)-17-[(1,3-Dioxolan-2-yl)methyl]-3-methoxymorphinan hydrobromide, 5, $C_{21}H_{30}BrNO_3$. The reaction mixture was heated for 16 h and the white crystalline precipitate of **5** was obtained. Yield: 0.66 g (48.10%). Mp 282–284 °C, R_f: 0.662 (A) and 0.620 (B). ^{1}H NMR (d_6-DMSO): 9.03 (s, 1H); 7.02–7.04 (m, 1H); 6.75 (s, 1H); 6.68–6.70 (m, 1H), 4.80–4.82 (m, 1H), 3.84–3.89 (m, 2H); 3.78–3.81(m, 2H), 3.75 (m, 1H), 3.70 (s, 3H); 2.85 (s, 1H); 2.80 (s, 1H); 2.75–2.77 (m, 1H); 2.53–2.56 (m, 1H); 2.42–2.50 (m, 1H); 1.88–1.93 (m, 1H); 1.65–1.73 (m, 2H); 1.53–1.61 (m, 1H); 1.46–1.49 (m, 1H); 1.33–1.36 (m, 2H), 1.20–1.29 (m, 3H),

1.14–1.17 (m, 1H), 0.89–0.96 (m, 1H). ^{13}C NMR (d_6-DMSO): 158.07, 141.79, 130.64, 128.98, 115.76, 110.75, 103.08, 64.70, 59.45, 55.21, 54.59, 46.75, 44.39, 38.48, 37.85, 37.54, 24.74, 23.93, 22.21, 20.54. MS: calcd for $C_{21}H_{29}NO_3$ 343.4631; found 343.4634, [M+H]$^+$ 344.46.34. Anal calcd C, 59.43; H, 7.13; N, 3.30; O, 11.31; Br, 18.83; found C, 59.18; H, 7.07; N, 3.28; O, 11.22; Br, 19.25.

2.1.2.6. (9α,13α,14α)-17-[2-(1,3-Dioxolan-2-yl)ethyl]-3-methoxmorphinan, 6, $C_{22}H_{31}NO_3$. The reaction mixture was heated for 13 h and the white crystalline precipitate of **6** was obtained. Yield: 0.80 g (56.10%). Mp 107–109 °C, R_f: 0.395 (A) and 0.473 (B). ^{1}H NMR (d_6-DMSO): 7.01–7.03 (m, 1H); 6.74 (s, 1H); 6.67–6.69 (m, 1H), 4.81–4.84 (m, 1H), 3.85–3.88 (m, 2H); 3.74–3.76(m, 2H), 3.73 (m, 1H), 3.69 (s, 3H); 2.85 (s, 1H); 2.80(s, 1H); 2.76–2.77 (m, 1H); 2.53–2.56 (m, 1H); 2.42–2.47 (m, 1H); 2.32–2.46 (m, 1H); 1.85–1.92 (m, 1H); 1.60–1.70 (m, 3H); 1.53–1.58 (m, 1H); 1.45–1.48 (m, 1H); 1.33–1.37(m, 2H), 1.22–1.30(m, 3H), 1.15–1.19(m, 1H), 0.93–1.02 (m, 1H). ^{13}C NMR (d_6-DMSO): 157.82, 141.23, 129.51, 128.43, 110.97, 110.53, 102.56, 64.16, 55.53, 54.87, 49.54, 44.94, 44.59, 41.67, 39.53, 37.40, 36.01, 32.07, 26.39, 26.06, 23.76, 21.96. MS calcd for $C_{22}H_{31}NO_3$ 357.2304; found 357.2307, [M+H]$^+$ 358.2380. Anal calcd C, 73.91; H, 8.74; N, 3.92; O, 13.43; found C, 73.90; H, 8.74; N, 3.92; O, 13.44.

2.1.2.7. (9α,13α,14α)-17-(2-Oxobutyl)-3-methoxymorphinan hydrobromide, 7, $C_{21}H_{30}BrNO_2$. The reaction mixture was heated for 16 h and the white crystalline precipitate of **7** was obtained. Yield: 0.63 g (48.30%). Mp 184–187 °C, R_f: 0.539 (A) and 0.506 (B). ^{1}H NMR (d_6-DMSO): 9.40–9.64 (d, 1H); 7.11–7.14 (d, 1H); 6.82–6.84 (m, 2H); 4.62–4.75 (m, 1H); 4.51–4.52 (m, 1H); 3.73 (s, 3H); 3.62 (s, 1H); 3.14–3.27 (m, 2H); 2.95–3.11 (m, 1H); 2.52–2.58(m, 2H), 2.38–2.50 (m, 1H), 2.38–2.58 (m, 1H); 2.13–2.21 (m, 1H); 1.87–2.03 (m, 1H); 1.60–1.63 (m, 1H); 1.49–1.52 (m, 2H); 1.27–1.43 (m, 3H); 1.04–1.18 (m, 1H); 0.98–1.02 (m, 3H); 0.86–0.96 (m, 1H). ^{13}C NMR (d_6-DMSO): 204.19, 158.54, 141.72, 130.87, 128.55, 115.56, 110.75, 62.98, 59.37, 55.45, 52.98, 46.74, 38.42, 37.89, 37.19, 32.83, 24.78, 23.94, 22.80, 20.74, 7.89. MS: calcd for $C_{21}H_{29}NO_2$ 327.2198; found 327.2202; [M+H]$^+$ 328.2275. Anal calcd C, 61.76; H, 7.40; N, 3.43; O, 7.84; Br, 19.57; found C, 61.80; H, 7.40; N, 3.43; O, 7.86; Br, 19.51.

2.1.2.8. (9α,13α,14α)-17-[(4,5-Dihydro-1H-imidazol-2-yl)methyl]-3-methoxymorphinan hydrobromide, 8, $C_{21}H_{30}BrN_3O$. The reaction mixture was heated for 16 h and the white crystalline precipitate of **8** was obtained. Yield: 0.52 g (38.10%). Mp 170–172 °C, R_f: 0.429 (A) and 0.663 (B). ^{1}H NMR (d_6-DMSO): 10.02 (s, 1H); 7.09–7.11 (m, 1H); 6.78–6.81 (m, 2H); 3.89 (s, 3H); 3.72–3.82 (m, 8H); 2.86–2.98 (m, 3H); 2.41–2.45 (m, 2H); 2.03–2.04 (m, 1H); 1.87 (s, 1H); 1.60–1.63 (m, 1H); 1.50–1.53 (m, 1H); 1.27–1.44 (m, 4H); 1.13–1.20 (m, 1H); 0.95–0.98 (m, 1H). ^{13}C NMR (d_6-DMSO): 161.68, 158.44, 141.79, 130.18, 128.31, 115.56, 110.79, 59.34, 55.26, 52.98, 50.09, 49.36, 48.56, 46.72, 38.41, 37.86, 37.50, 24.79, 23.97, 22.21, 20.98. MS: calcd for $C_{21}H_{29}N_3O$ 339.2709; found 339.2705; [M+H]$^+$ 340.2715. Anal calcd C, 60.00; H, 7.19; N, 10.00; O, 3.81; Br, 19.01; found C, 59.60; H, 7.17; N, 9.95; O, 3.80; Br, 19.48.

2.1.3. Synthesis of N-alkylated dextromethorphan derivative compound 4 (method B)

2 mmol of **1** dissolved in 3 ml DMSO was cooled down in ice bath and 0.2 g 1.45 mmol of anhydrous potassium carbonate was added. 0.5 ml of 30% solution of hydrogen peroxide was added dropwise and after 30 min of mixing on a magnetic stirrer 9 ml of water was added. The obtained precipitation was filtered and washed with water.

2.1.3.1. 2-[(9α,13α,14α)-3-Methoxymorphinan-17-ylacetamide, 4, $C_{19}H_{26}N_2O_2$.
Yield: 0.22 g (35.00%). Mp 78–80 °C, R_f: 0.729 (A) and 0.650 (B). ^1H NMR (d_6-DMSO): 7.70–7.76 (m, 1H), 7.10–7.14 (m, 1H); 6.81–6.83 (m, 2H); 4.00–4.34 (m, 2H); 3.72 (s, 4H); 3.25–3.30 (m, 1H), 3.11–3.16 (m, 1H); 2.98–3.04 (m, 1H); 2.77–2.84 (m, 1H); 2.43–2.46 (m, 1H); 2.14–2.38 (m, 1H); 1.90–1.98 (m, 1H); 1.58–1.61 (m, 1H); 1.40–1.52 (m, 3H); 1.25–1.36 (m, 2H); 1.10–1.17 (m, 1H); 0.91–0.95 (m, 1H). ^{13}C NMR (d_6-DMSO): 168.72, 158.57, 138.72, 129.27, 125.73, 112.16, 110.64, 58.47, 55.07, 52.46, 46.79, 39.53, 38.37, 35.68, 34.77, 27.94, 25.03, 23.39, 21.44. MS: calcd for $C_{19}H_{26}N_2O_2$ 314.4219; found 314.1999, [M+H]$^+$ 315.2072. Anal calcd C, 72.58; H, 8.33; N, 8.91; O, 10.18; found C, 72.56; H, 8.33; N, 8.92; O, 10.19.

2.1.4. Synthesis of N-alkylated dextromethorphan derivatives compound 9 (method C)
0.51 g (2 mmol) of 3-methoxymorphinan and 10 ml of vinyl ketone was cooled down in ice bath and 0.4 ml of Triton B was added at temperature of 0–5 °C. The reaction mixture was stirred on a magnetic stirrer for 3 h. 50 ml of diethyl ether was added and ethereal solution was decanted and the obtained precipitate was filtered and washed with diethyl ether.

2.1.4.1. (9α,13α,14α)-17-(3-Oxobutyl)-3-methoxymorphinan hydrobromide, 9, $C_{21}H_{30}BrNO_2$.
Yield: 0.15 g (23.10%). Mp 140–142 °C, R_f: 0.539 (A) and 0.550 (B). ^1H NMR (d_6-DMSO): 9.19–9.35 (m, 1H); 7.12–7.14 (m, 1H); 6.82–6.84 (m, 2H); 3.73 (s, 3H); 3.69 (s, 1H); 3.54–3.55 (m, 1H); 3.14–3.23 (m, 1H); 3.12 (s, 1H); 3.04–3.09 (m, 1H); 2.98–3.02 (m, 2H); 2.93–2.95 (m, 1H); 2.63–2.70 (m, 1H); 2.32–2.44 (m, 1H); 2.17 (s, 3H); 2.00–2.03 (m, 1H); 1.81–1.88 (m, 1H); 1.61–1.63 (m, 1H); 1.46–1.52 (m, 3H); 1.24–1.35 (m, 2H); 1.12–1.18 (m, 1H); 0.87–0.99 (m, 1H). ^{13}C NMR (d_6-DMSO): 208.97, 158.12, 141.79, 130.18, 128.31, 115.50, 110.76, 59.37, 55.23, 48.21, 47.96, 46.76, 41.59, 38.44, 37.76, 37.18, 30.67, 24.79, 23.91, 22.22, 20.98. MS: calcd for $C_{21}H_{29}NO_2$ 327.2198; found 327.2202; [M+H]$^+$ 328.2275. Anal calcd C, 61.76; H, 7.40; N, 3.43; O, 7.84; Br, 19.57; found C, 61.60; H, 7.37; N, 3.40; O, 7.82; Br, 19.81.

2.2. In vitro assay

2.2.1. Cell lines and culture
The KXα3β4R2 (expressing rat α3β4 nAChRs) cell lines have been previously described.[19] The cell lines were maintained in MEM supplemented with 10% FBS, 100 units/ml penicillin G, 100 mg/ml streptomycin and 0.7 mg/ml geneticin at 37 °C with 5% CO_2 in a humidified incubator.

2.2.2. Whole-cell current recording α3β4 nAChRs
Whole cell current was measured using EPC 10 HEKA Instruments amplifier. All drugs were applied by fast perfusion system (DynaFlow, CelletriconAB, Mölndal, Sweden) with 16 channels chip. Cells were clamped at 60 mV holding potential. KXα3β4R2 cells were collected at 70% confluence and suspended in HEPES [10 mM, pH 7.4] containing 120 mM NaCl, 3.1 mM KCl, 2 mM $CaCl_2$, 5 mM glucose at room temperature. The glass pipettes with 5–7 MΩ resistance were filled with HEPES [10 mM, pH 7.2], containing 145 mM CsCl, 1 mM $MgCl_2$, 2 mM ATP, 1 mM EGTA. All experiments were performed under Visual control using an Olympus CKX41 inverted microscope (Olympus Corporation). Test compounds were applied at concentrations of 0.1, 1, 10, and 100 nM, 1, 10 and 100 μM in the absence of (S)-nicotine for stimulation or in the presence of 100 μM (S)-nicotine for inhibition measurements. For inhibition studies, the decrease in current relative to 100 μM (S)-nicotine (100%) was determined. Raw data was collected using PatchMaster Version 2.32 software (Celletricon AB) and analysed

using GraphPad Prism Version 5.0 software (GraphPad Software, Inc., La Jolla, CA, USA).

2.3. Molecular modeling

2.3.1. Homology models
The sequences data for the α3 and β4 nAChRs subunits were obtained from the UniProt database implemented in ExPASy Bioinformatics Resource Portal.[20] The cryo-electron microscopy structure of the Torpedo nAChR determined at ~4 Å resolution (PDB ID: 2BG9) was used as a template. Sequence alignment of the whole Torpedo nAChR (i.e., α1, α1, β1, γ, and δ) as well as human (h) α3 and β4 nAChRs subunits was performed using ClustalW2 Server.[21] Two α1 subunits in the Torpedo template were used to build two α3 subunits in the target, whereas β1, γ, and δ in the template were used to construct three β4 subunits in the target. Modeller 9.9[22] was used to obtain the population of 100 homology models of human α3β4 nAChR. The best model was subjected to model quality assessments, using the MOE Molecular Environment module for Ramachandran plots (http://www.chemcomp.com/software.htm) and the web-based tools of Annolea,[23] Verify3D[24] and ProCheck.[25]

2.3.2. Molecular docking and molecular dynamics
DM derivatives were optimized using HF approximation and 6-31G basis set of Spartan 10 V.1.1.0 (Wavefunction, Inc. Irvine, CA 92612 USA). Spartan was also used to calculate electrostatic potential. Tautomerization and protonation state at physiological pH were assessed with LigPrep[26] and Epik[27] modules of Schrödinger suite of software. Molecular docking was performed with Glide. The docking space (i.e., Grid definition) covered the ion channel of studied nAChR model and was selected based on the experimental evidence.[19] Molecular docking was performed with Glide using standard precision (SP) protocol. The complexes subjected to molecular dynamic (MD) simulations with Desmond v. 3.0.3.1[28] were selected based on the visual inspection rationalised by earlier studied on dextromethorphan binding mode in the α3β4 nAChR.[6] Ligand-receptor complexes were inserted into POPC membrane and solvated with water. Ions were added to neutralize protein charges and to the concentration of 0.15 M NaCl. The complexes embedded in membrane were first minimized and then subjected to 1 ns MD in NVT ensemble, followed by 10 ns MD in NPT ensemble. Yasara Structure[29], PyMol v. 1.5.0.3[30] and MOE Molecular Environment were also used for visualization of results.

2.4. Behavioral studies

2.4.1. Animals
The experiments were carried out on naïve male Wistar rats weighing 250–300 g (Farm of Laboratory Animals, Warszawa, Poland) or naïve male Swiss mice weighing 20–25 g (Farm of Laboratory Animals, Warszawa, Poland) at the beginning of the experiments. The animals were group-housed, kept under standard laboratory conditions (12/12-h light/dark cycle) with free access to tap water, and adapted to the laboratory conditions for at least one week. The rats had limited access to lab chow (150 g per 8 rats on 24 h, given as a single meal in the evening) (Agropol, Motycz, Poland). The rats were handled once a day for 5 days preceding the experiments. Additionally, all efforts were made to minimize animal suffering and to use only the number of animals necessary to produce reliable scientific data. Each experimental group consisted of 7–14 animals. The experiments were performed between 9.00 a.m. and 5.00 p.m. All experiments were carried out according to the National Institute of Health Guidelines for the Care and Use of Laboratory Animals and the European Community Council Directive of 24 November 1986 for Care and Use of Laboratory Animals (86/609/EEC), and approved by the local ethics committee.

2.4.2. Drugs

The compounds tested were: (−)-nicotine hydrogen tartrate (Sigma, St. Louis, MO, USA), dextromethorphan (DM), and compounds **1**, **5** and **6** (see Fig. 3 and Table 1). The selection of the compounds for behavioural studies was connected with the easiness and yield of the synthesis as well as with the idea to explore the spectrum of in vivo effects of compounds with different in vitro activity. All agents were dissolved in saline (0.9% NaCl). The pH of the nicotine solution was adjusted to 7.0. Compounds **1**, **5** and **6** (1/10 and 1/20 LD_{50} previously established) were suspended in one drop of 1% solution of Tween 80 (Sigma, St. Louis, MO, USA) and diluted in saline. Fresh drug solutions were prepared on each day of behavioral testing. All agents were administered intraperitoneally (ip) in a volume of 5 ml/kg (rats) or 10 ml/kg (mice) and, except for nicotine, drug doses refer to the salt form. Control groups received vehicle injections at the same volume and via the same route of administration.
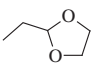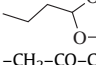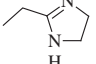
The doses of nicotine and DM were chosen based on literature data,[31–33] whereas the doses of new compounds were chosen based on preliminary studies.
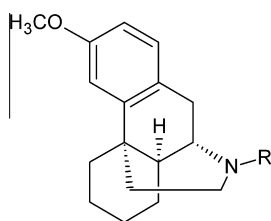
The general behaviors of the mice were observed continuously for 1 h after the treatment and intermittently for 4 h during a period of 24 h. All mice were further observed for any signs of toxicity, deaths, and the latency of death during a period of one week. The toxicity of the studied compounds was comparable to dextromethorphan which is: LD_{50} in rats 350 mg/kg[34] and LD_{50} in mice 39 mg/kg.[35] The studied derivatives most probably hit the same off-targets as dextromethorphan, that is, NMDA receptor (it was confirmed experimentally and will be published elsewhere) and sigma receptor.

2.4.3. Apparatus

2.4.3.1. Conditioned place preference (CPP).
Each of six rectangular boxes (60 cm × 35 cm × 30 cm) was divided into three compartments: two large compartments (20 cm × 35 cm) were separated by removable guillotine doors from a small central area (10 cm × 10 cm). The compartments were differentiated by both visual and tactile cues: one was white with a grooving on the black floor, another was black with wire mesh on the white floor. The central, small grey area served as connection and a start compartment. The testing boxes were kept in a soundproof room with neutral masking noise and a dim 40-l× illumination.

2.4.3.2. Locomotor sensitization.
Locomotion was recorded individually in round actometer cages (32 cm in diameter; Multiserv, Lublin, Poland) kept in a sound-attenuated experimental room. Two photocell beams located across the axis measured the animal's movement automatically.

2.4.4. Procedures

2.4.4.1. Influence of dextromethorphan and compounds 1, 5 and 6 on the expression of nicotine-induced CPP in rats.
The place conditioning experiment (unbiased design) consisted of pre-conditioning, conditioning and post-conditioning phases. For pre-conditioning (Day 1), each animal was placed separately in the neutral area with the guillotine doors removed to allow access to the entire apparatus. The amount of time the rats spent in each of the two large compartments was measured (a baseline preference), and observed on a monitor through a video camera system for 15 min. Rats that showed a preference for one of the compartments were considered not to be neutral in preference for either side and were excluded from further study (less than 5% of rats).

The conditioning phase consisted of 30 min sessions, two per day. In the morning sessions, the rats were injected with vehicle and confined in one compartment, whereas on afternoon sessions, they received injections of nicotine (0.175 mg/kg, base, ip) and were then confined in the opposite compartment. Sessions were conducted twice each day with an interval of 6–8 h for 3 consecutive days (Days 2–4). Injections were administered immediately before confinement in one of the two large compartments, as mentioned above. Control group received vehicle every day.

On Day 5, conducted one day after the last conditioning trial, animals were placed in the neutral area with the guillotine doors removed and allowed free access to all compartments of apparatus for 15 min. The time spent in the vehicle- and drug-paired compartments was recorded for each animal. To evaluate the effects of DM and tested compounds on the expression of nicotine-induced CPP, on this post-conditioning phase, rats pretreated with vehicle were injected with vehicle ($n = 7$) or nicotine (0.175 mg/kg, ip, $n = 8$) and rats pretreated nicotine (during conditioning, as mentioned above) were injected with nicotine (0.175 mg/kg, ip, $n = 10$), and DM (5 mg/kg, $n = 7$ and 10 mg/kg, $n = 7$) or compounds **1** (1/10, $n = 7$ or 1/20 LD_{50}, $n = 7$), **5** (1/10, $n = 8$ or 1/20 LD_{50}, $n = 7$) and **6** (1/10, $n = 8$ or 1/20 LD_{50}, $n = 7$), 60 min before nicotine injection and were immediately tested for the expression of CPP.

2.4.4.2. Influence of DM, compounds 1, 5 and 6 on the expression of nicotine-induced locomotor sensitization in mice.
This method was similar to that used in our previous experiments accordingly to the data indicating that at the dose of 0.175 mg/kg nicotine produces robust locomotor sensitization in mice under our laboratory conditions.[33] During the pairing phase (days 1–9), mice received the following injections: vehicle (ip) + vehicle (sc) or vehicle (ip) + nicotine (0.175 mg/kg, sc) every other day for five sessions.

The mice remained drug free for one week and, on the challenge day (Day 16), the mice pretreated with vehicle were challenged with nicotine (0.175 mg/kg, sc $n = 8$) and the mice pretreated with nicotine (as mentioned above) were further challenged with nicotine (0.175 mg/kg, sc, $n = 8$) or DM (5 mg/kg, $n = 8$ and

Table 1
The investigated dextromethorphan derivatives and their effect on the (S)-nicotine-induced current in KXα3β4R2

Dextromethorphan derivatives	Substituents (R)	IC_{50} (μM)
1	–CH$_2$–CN	10.47 ± 1.67
2	–CH$_2$–CH$_2$–CN	176.00 ± 1.1
3	–CH$_2$–CH$_2$–CH$_2$–CN	87.00 ± 1.12
4	–CH$_2$–CO–NH$_2$	41.40 ± 1.14
5		1.95 ± 0.13
6		7.14 ± 1.0
7	–CH$_2$–CO–CH$_2$–CH$_3$	2.50 ± 0.19
8		6.61 ± 1.06
9	–CH$_2$–CH$_2$–CO–CH$_3$	2.57 ± 0.18
Dextromethorphan (DM)	–CH$_3$	11.05 ± 1.08
Nordextromethorphan (NORDM)	–H	3.08 ± 1.03

10 mg/kg, $n = 10$) and compounds **1** (1/10, $n = 8$ or 1/20 LD$_{50}$, $n = 10$), **5** (1/10, $n = 8$ or 1/20 LD$_{50}$, $n = 10$) and **6** (1/10, $n = 8$ or 1/20 LD$_{50}$, $n = 9$), 60 min before nicotine challenge injection. Locomotor activity was recorded for 60 min during the pairing phase (days 1–9) and on the 16th challenge test, immediately after injections.

2.4.5. Statistical analysis

For the CPP paradigm, the results are expressed as scores, that is, the differences (in s) between post-conditioning and pre-conditioning time spent in the drug-associated compartment (means ± SEM). The data were analyzed by the analysis of variance (ANOVA). Locomotor activity was expressed as a number of photocell beam breaks (means ± SEM). For locomotor sensitization, data were analyzed using repeated measure analysis of variance (ANOVA) with treatment as independent factor and days as repeated measures. The response to drugs on the challenge day was compared using one-way ANOVA. Post-hoc comparison of means was carried out with the Tukey's test for multiple comparisons, when appropriate. The confidence limit of $p < 0.05$ was considered statistically significant.

3. Results and discussion

3.1. Chemistry

Compound **1** was previously obtained in the reaction of DM and trimethylcyanosilane.[36,37] These studies were aimed to oxidize tertiary amines and alkaloids through monoelectronic transfer. The pharmacological activity of compound **1** has been not determined. Compound **2**, obtained from commercial sources was found to inhibit DM binding sites in guinea pig brain homogenates with IC$_{50}$ of 775 nM.[38]

Compounds **9** has been designed by our research group as NCI of nAChRs using computer based model[39] but it has been never synthesized. Compounds **3–8** have not been described yet in the available literature.

Demethylation of DM was performed using Peete's method (Fig. 2).[40] All the compounds **1–9** were obtained from demethylated DM using various alkylating agents (Fig. 3).

3.2. Pharmacological activity

It has been previously reported that DM presents a non-competitive inhibitory activity toward α3β4 nAChRs, with 20 times higher binding affinity than levomethorphan to the hydrophobic cleft the two enantiomers bind.[16,17,38] In this regard, the effect of studied compounds on the function of the α3β4 nAChRs was evaluated using patch-clamp technique in the whole-cell configuration. The compounds were first examined for their ability to induce current activation at the range of 0.1–100 μM concentrations. No measurable response was observed at any tested concentration, data not shown. The ability of the test compounds to affect (S)-nicotine-induced current was assessed using 100 μM (S)-nicotine and appropriate concentration range of studied dextromethorphan derivatives. Compound **5**, **7** and **9** as well as nordextromethorphan (NORDM) induced ∼3–6-fold higher inhibitory activity on (S)-nicotine-induced currents (IC$_{50}$ values of 1.95, 2.50, 2.57, and 4.26 μM, respectively; see Table 1 and Fig. 4) compared to dextromethorphan (DM) (IC$_{50}$ = 12.87 μM). Furthermore, compounds **1**, **6**, and **8** produce suppression of (S)-nicotine-induced current comparable to DM (Table 1). The application of compound **2** and **3** had no significant effect on the (S)-nicotine-induced currents (IC$_{50}$ values of 176 and 87 μM, respectively; see Table 1) indicating that both compounds do not produce any effect on the α3β4 nAChRs.
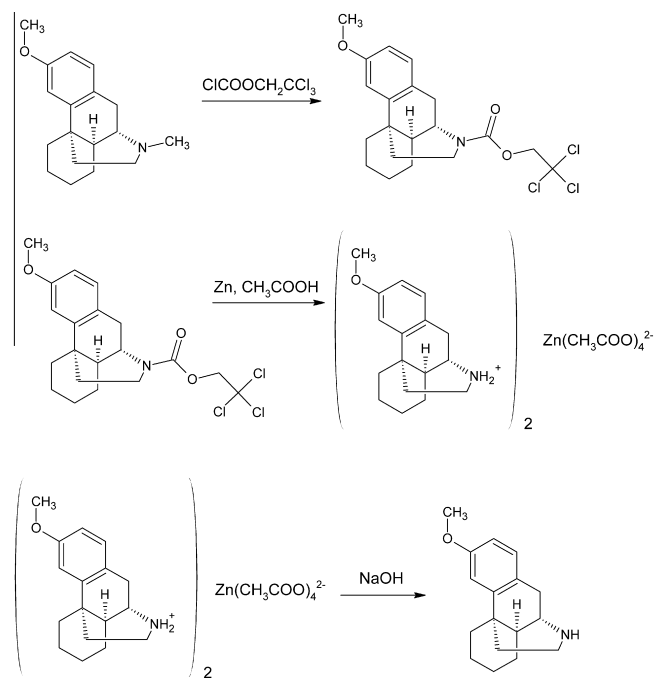

Figure 2. Demethylation of dextromethorphan.

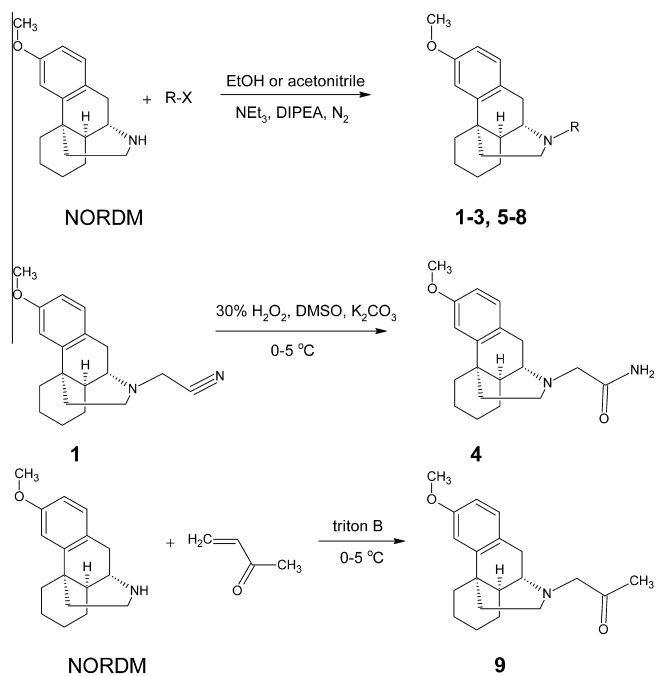**Figure 3.** Synthesis of compounds **1–9**.

3.3. Molecular modeling

3.3.1. Homology modeling and model quality assessment

The sequence identity of the α3 and β4 subunit was ∼45–55% comparing to each subunit of *Torpedo* nAChR. Homology models were assessed considering their Discrete Optimized Protein Energy (DOPE) profiles. The best model was subjected to model quality assessments, using the following tools: MOE Molecular Environment module for Ramachandran plots and the web-based tools of Annolea,[23] Verify3D[24] and ProCheck.[25]
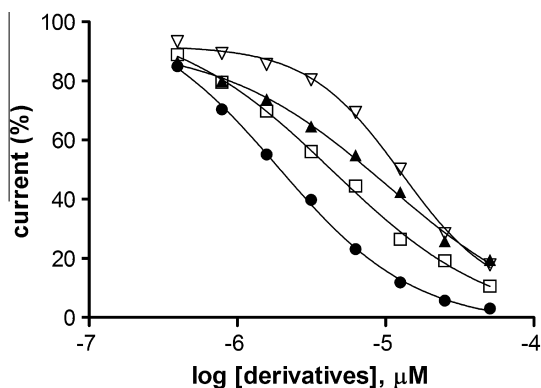
Figure 4. The effect of the concentration of dextromethorphan (▽), nordextromethorphan (□) as well as compound **5** (●), and **9** (▲) on the (*S*)-nicotine-induced current in KXα3β4R2 cells determined using whole-cell configuration of the patch-clamp technique. The calculated IC$_{50}$ values are included in the Table 1.

3.3.2. Ligand–receptor interactions

The studied non-competitive antagonists interact with the transmembrane region of the α3β4 nAChR, which consists of five subunits (i.e., two α3 and three β4), each composed of M1–M4 transmembrane segments. Among the transmembrane segments, M2 is relatively more hydrophilic and thus, it tends to face the center of the ion channel.[41] The amino acid sequences in M2 are highly conserved among different subunits and species, forming a series of amino acid rings exposed to the center of the pore and distributed along the axis of the channel.[41] In the considered ion channel, the amino acid rings in each α3/β4 subunit are named: outer or extracellular (position 20′), nonpolar (position 17′), PHE/VAL (position 13′), LEU (position 9′), SER (position 6′), THR (position 2′), intermediate (position −2′), and cytoplasmic or inner (position −5′). Accordingly, each β4 subunit carries important change in comparison to most α and non-α nAChR subunits:[41] that is, phenylalanine that are located at position 13′ instead of valine residues.

All the studied compounds have a positively charged nitrogen atom. This feature enables them to be attracted by the negatively charged residues at the extracellular mouth (i.e., at 20′ position) which results in pulling in the molecule into the ion channel. In addition, within the binding pocket located deeper in the ion channel (close to position 13′) there is the β4-Phe255 residue that may participate in the cation-π interactions with the protonated nitrogen. However, the docking results suggested that the protonated nitrogen atom of studied compounds as well as N-substituted moieties are directed toward the polar ring formed by serine (at position 6′) residues. Cation–π interaction energies are of the same order of magnitude as hydrogen bonds or salt bridges and in the considered case hydrogen bonds were favored.

In particular, each ligand interacts with the middle portion of the ion channel between residues that form PHE/VAL (at position 13′) and SER (at position 6′) rings (see Fig. 5 and 7) by van der Waals interactions as well as hydrogen bonding. More specifically, DM interacted with β4-Phe255 and α3-Val254 at position 13′, β4-Ala252 and α3-Ser251 at position 10′, β4-Leu251 and α3-Leu250 at position 9′, as well as with β4-Ser248 at position 6′ (Fig. 5).
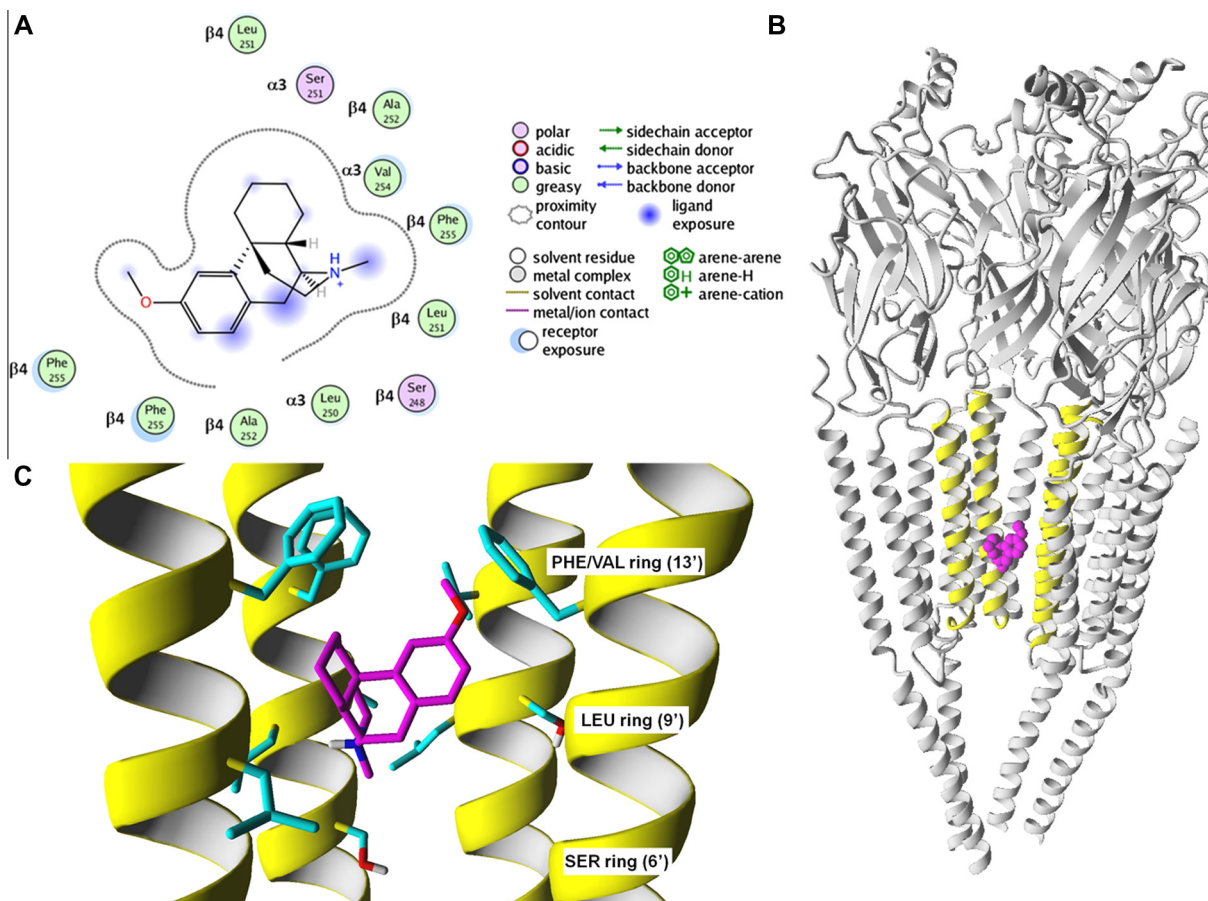

Figure 5. DM molecule in the binding site of α3β4 nAChR model. (A) Scheme of interactions; (B) Side view of the whole model showing the ligand (magenta) docking site; (C) Detailed view of the luminal site (i.e., within the ion channel) that is located between PHE/VAL (at position 13′) and SER (at position 6′) rings. Residues involved in ligand binding are shown explicitly in stick mode (element coded mode). DM is rendered in ball (B) or stick (C) mode. For clarity, one β4 subunit is hidden, whereas the M2 segments are show in yellow. All non-polar hydrogen atoms are hidden.
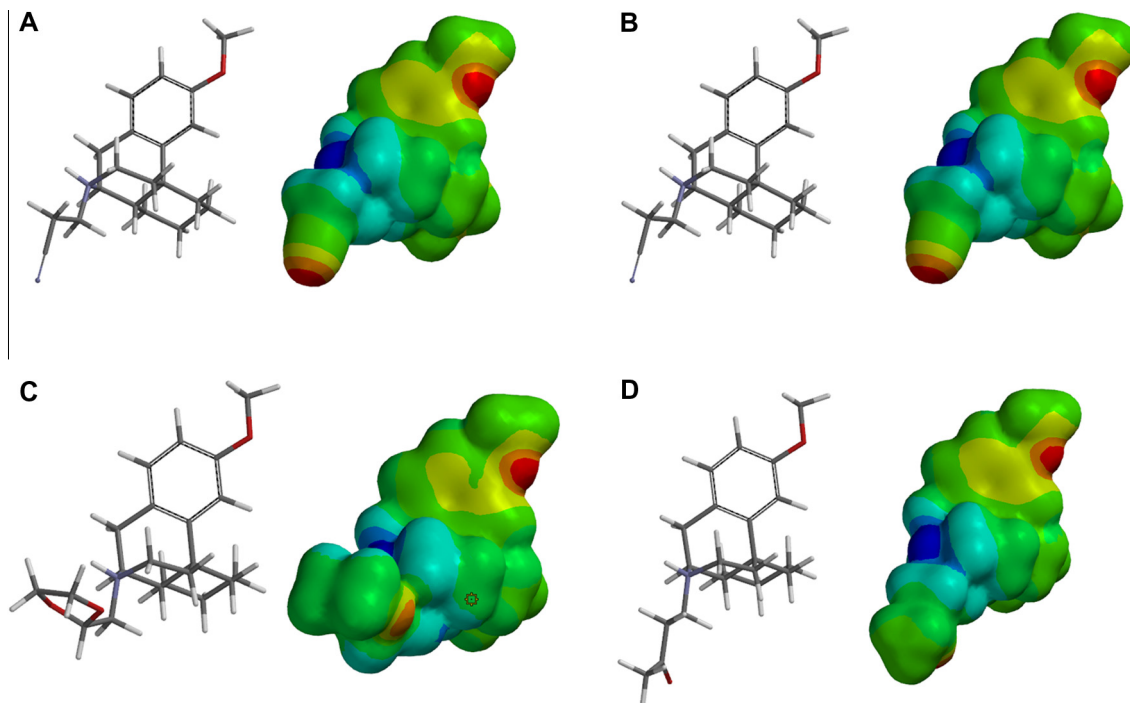
Figure 6. The map of electrostatic potential distribution for inactive compounds **2** (A), **3** (B) and active compounds **5** (C) and **9** (D).
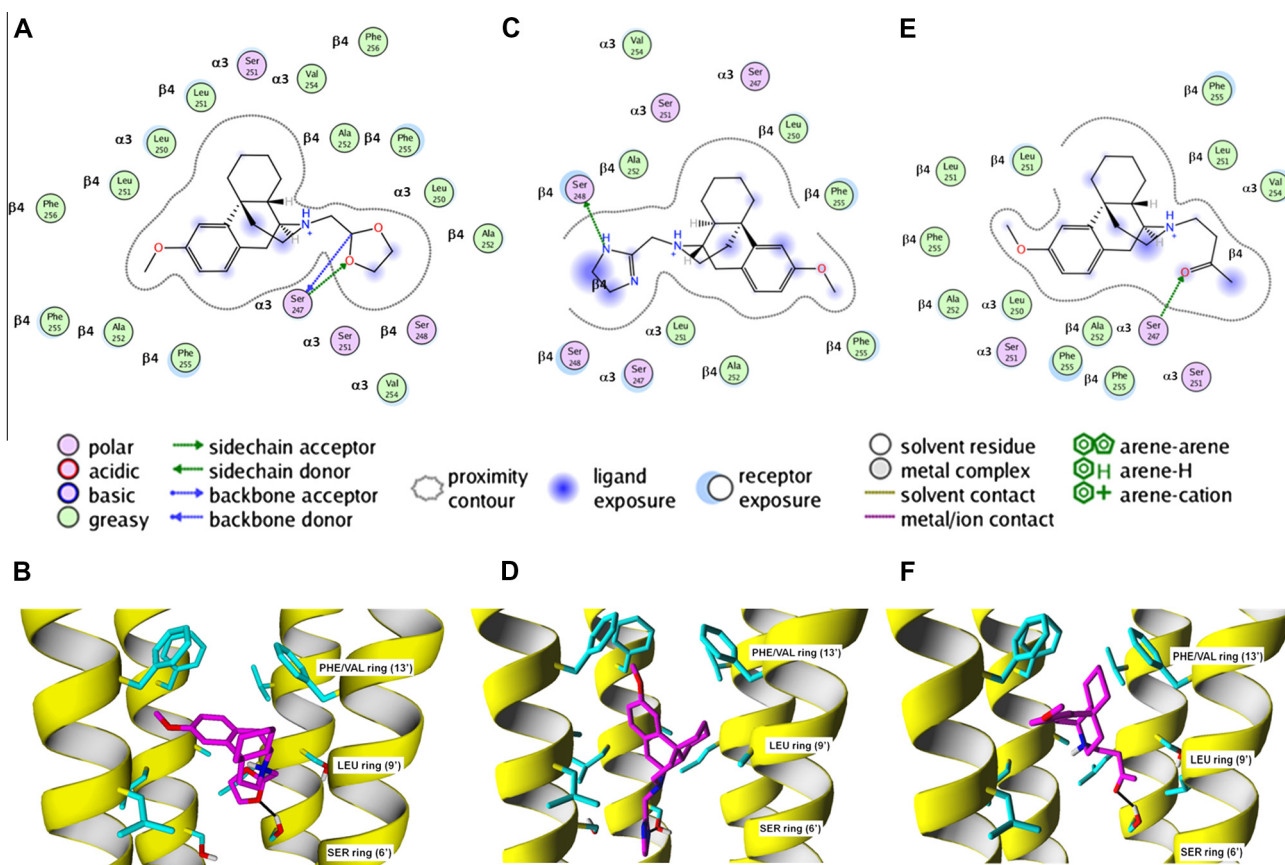

Figure 7. DM derivatives, including compounds **5**, **8** and **9** (shown in magenta) in the binding site within the ion channel of α3β4 nAChR model. (A and B) show the scheme interactions and detailed view of compound **5** binding site, respectively. This ligand is stabilized in the binding pocket by hydrogen bond interaction, formed between dioxolane oxygen of the ligand and the hydroxyl group of α3-Ser247; (C and D) present the scheme interactions and detailed view of compound **8** binding site, respectively. In addition, this ligand is also stabilized in the binding pocket by hydrogen bond interaction, formed between the nitrogen from imidazole ring of compound **8** and hydroxyl group of the β4-Ser248; (E and F) depict the scheme interactions and detailed view of compound **9** binding site, respectively. Moreover, this ligand is stabilized in the binding pocket by hydrogen bond interaction, formed between carbonyl oxygen of 3-oxo-butyl moiety of the ligand and hydroxyl group of α3-Ser247. For (B, D, and F) the residues involved in ligand binding are shown explicitly in stick mode (element coded mode). Each compound is rendered in stick mode and colored in magenta. For clarity, one β4 subunit is hidden, whereas the M2 segments are show in yellow. All non-polar hydrogen atoms are hidden.
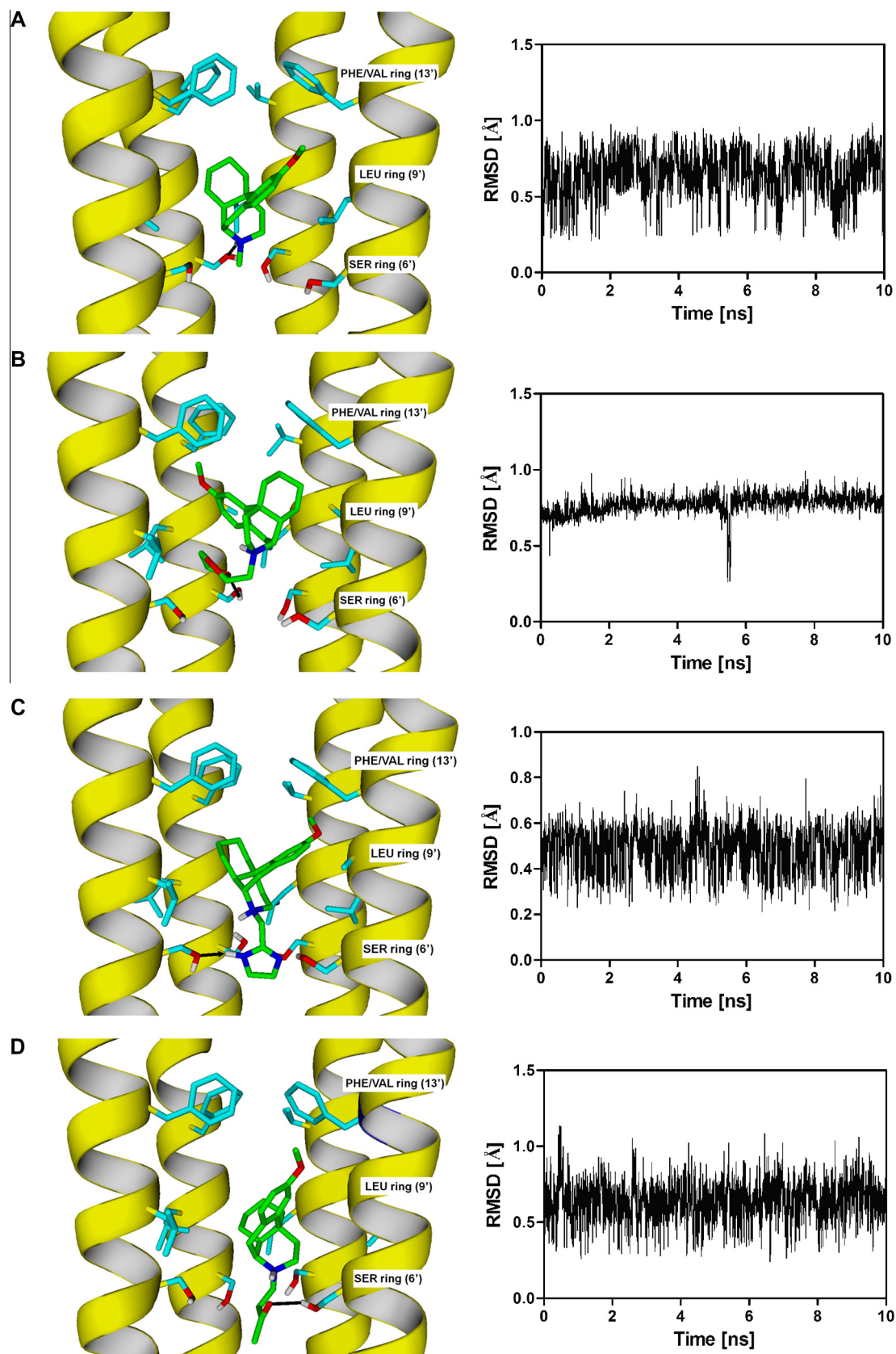
Figure 8. DM derivatives complexes with the α3β4 nAChR models obtained after the MD simulation for DM (A) and compounds **5** (B), **8** (C), and **9** (D) (shown in green) as well as the RMSD values calculated during the MD run for each mentioned before complex. Each ligand is stabilized in the binding pocket by hydrogen bond interaction, formed between the protonated nitrogen (A), dioxolan oxygen (B), the nitrogen from imidazol-2-yl ring (C) or the carbonyl oxygen of 3-oxo-butyl moiety and the hydroxyl group of β3-Ser248, respectively. See Figure 7 for other details.

However, the docking results for DM derivatives (i.e., compounds **5**, **8** and **9**) suggest that they interact with the same residues as indicated for DM, and these ligands are stabilized by additional hydrogen bonding. In particular, for compound **5** hydrogen bond is formed between oxygen of dioxolane moiety of the ligand and hydroxyl group of α3-Ser247 (see Fig. 6). However, compounds **8** and **9** are stabilized by hydrogen bonds, formed between the nitrogen from imidazole ring of compound **8** and hydroxyl group of the β4-Ser248 and between the carbonyl oxygen of 3-oxo–butyl moiety of compound **9** and hydroxyl group of the α3-Ser247 (see Fig. 7). These α3-Ser247 and β4-Ser248 are located on the same level in the channel model and equivalent in molecular docking experiment and it is impossible to point out that only one of these serine residues is responsible for interactions with the channel blocker. Indeed, clusters of docking poses where ligands interacted with either α3-Ser247 or β4-Ser248 were obtained and the final pose for a particular ligand was selected based on Glide scoring and visual inspection. The poses of compounds **6** and **7** are similar to those of compounds **5** and **9**.

Molecular docking results do not make it possible to explain the weak activity of compounds **2** and **3**. However, the maps of electrostatic potential distribution (Fig. 6A and B, respectively) show that in these derivatives the cyano group bears a strong partial negative charge which is unfavorable regarding negative charge of amino acid ring (position 20′) at the entrance of the channel. In the case of other derivatives (e.g., compound **5** and **9**, Fig. 6C and D, respectively), the molecules do not exhibit highly negative charged regions and may be easier attracted into the ion channel. In general, nAChR ion channels are cation-selective and accommodate better compounds with a balanced positive charge.

The molecular dynamics simulations showed that the obtained ligand–receptor complexes were stable regarding potential energy (Fig. 8). Moreover, ligand RMSD between starting and final complexes after 10 ns MD was in the range of 0.21–1.47 Å which additionally confirms that the modeled complexes were stable. After

MD run it turned out that the interactions with β4-Ser248 are favored over interactions with α3-Ser247 (Fig. 8).

3.4. Behavioral effects of selected derivatives

3.4.1. Influence of DM and compounds 1, 5 and 6 on the expression of nicotine-induced CPP in rats

All rats showed no significant place preference for the drug-associated compartment before drug conditioning, which indicated that the CPP apparatus that we used was of a non-biased design.[42] Figure 9 indicated the effects of DM and compounds **1**, **5** and **6** on nicotine induced CPP [one-way ANOVA: $F(12,77) = 2.687$, $p = 0.048$]. Administration of nicotine (0.175 mg/kg, four conditioning sessions, days 2–4) induced a clear place preference, shown as significant increase in time spent in the drug-associated compartment during the post-conditioning test phase (Day 5, $p <0.001$, post hoc Tukey's test). Interestingly, post-hoc individual comparisons indicated a significant inhibitory effect of DM at a dose of 10 mg/kg ($p <0.01$) and compound **1** (1/20 LD$_{50}$, $p <0.05$) (Tukey's test) on nicotine-induced CPP. Both DM and new compounds do not induce significant changes in the place preference test at the applied doses when administered without nicotine (data not shown).

3.4.2. Influence of DM and compounds 1, 5, and 6 on the expression of nicotine-induced locomotor sensitization in mice

Concerning the locomotor response after administration of nicotine (0.175 mg/kg, sc) or saline during the pairing phase (Day 1 and Day 16—challenge), two-way ANOVA revealed a treatment effect [$F(11,166) = 20.05$, $p <0.0001$], a day effect [$F(1,166) = 19.92$, $p <0.0001$] with interaction between treatment and day [$F(11,166) = 13.28$, $p <0.0001$] (Fig. 10). On the Day 1, one-way ANOVA did not reveal any significant treatment effect [$F(11,94) = 1.254$, $p = 0.2660$]. However, on the Day 16, after an additional injection of nicotine, one-way ANOVA revealed a significant treatment effect [$F(11,94) = 2.797$, $p <0.0038$]. Indeed, after this last nicotine injection (challenge), a significant difference in response was observed when compared to either the first nicotine injection ($p <0.01$) or in response to nicotine in animals treated repeatedly with vehicle ($p <0.01$, Tukey's test). DM at the dose of 10 mg/kg and administered at both used doses before nicotine challenge dose, were effective in blocking the expression of nicotine sensitization
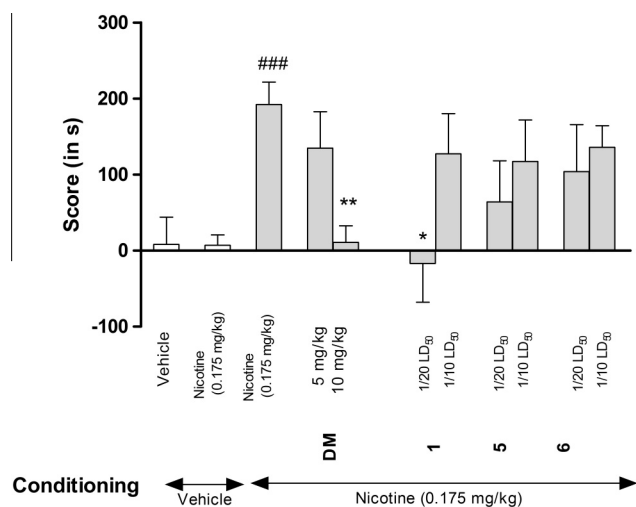

Figure 9. Effects of dextromethorphan (DM, 5 and 10 mg/kg, ip) and compounds **1**, **5**, and **6** (1/10 and 1/20 LD$_{50}$, ip) on the expression of nicotine-induced CPP. Place preference procedure consisted of pre-conditioning, three conditioning sessions with nicotine (0.175 mg/kg, ip) and post-conditioning test. During the post-conditioning phase, rats received injection of vehicle, nicotine (0.175 mg/kg), or DM (5 and 10 mg/kg) as well as compounds **1**, **5**, and **6** (1/10 or 1/20 LD$_{50}$) 60 min before nicotine injection (0.175 mg/kg), and were immediately tested for the expression of CPP. Data represent means ± SEM and are expressed as the difference (in s) between post-conditioning and pre-conditioning time spent in the drug-associated compartment. $n = 7$–14 rats per group; *$p <0.05$; **$p <0.01$ versus nicotine-conditioned group; ###$p <0.001$ versus vehicle-conditioned control group (Tukey's test).
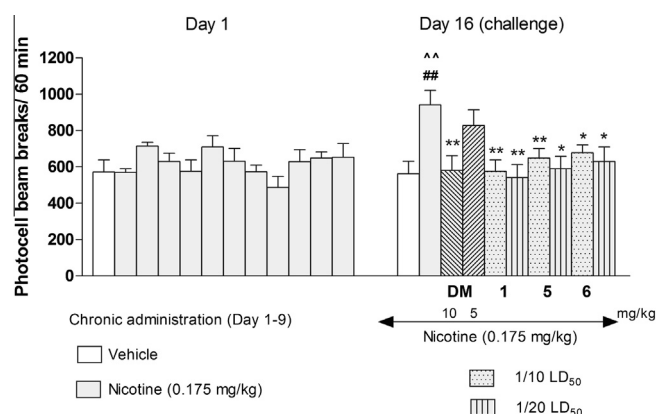

Figure 10. Effects of dextromethorphan (DM, 5 and 10 mg/kg, ip) and compounds **1**, **5**, and **6** (1/10 and 1/20 LD$_{50}$, ip) on the expression of locomotor sensitization to nicotine in mice. Nicotine (0.175 mg/kg, sc) or vehicle were injected daily for 9 days, every other day; on day 16 (a test for expression of sensitization) mice were given nicotine (0.175 mg/kg, sc) as well as DM or compounds **1**, **5**, and, **6**, 60 min before nicotine challenge injection. Data represent means ± SEM; $n = 8$–10 mice per group. ##$p <0.01$ versus the first pairing day; ^^$p <0.01$ versus vehicle-pretreated and nicotine-challenged mice; *$p <0.05$, **$p <0.01$, versus nicotine-pretreated and nicotine-challenged mice (Tukey's test).

(p <0.05 for compounds **5** and **6**, 1/20 LD$_{50}$; p <0.01 for other compounds, vs nicotine-pretreated and nicotine-challenged mice). Neither DM nor any compounds tested given acutely or repeatedly, significantly affected basal locomotor activity of mice (data not shown).

Compounds **5** and **6** were highly potent in vitro and were also effective in blocking the expression of the nicotine sensitization in mice. However, both compounds did not show any significant inhibitory effect on nicotine-induced CPP in rats. It might be due to the strain differences in drug metabolism. Moreover, different pathways as well as various brain areas are involved in CPP and locomotor sensitization.

In the case of compound **1**, which is effective at a dose of 1/20 LD$_{50}$ only, it follows the trend that a lower dose of all new compounds studied in vivo has greater inhibitory effect on nicotine-induced CPP even though only the effects elicited by compound **1** is statistically significant. This observation will be explored in more details and the results reported elsewhere.

4. Conclusions

In the present work we designed, synthesized and pharmacologically characterized novel non-competitive inhibitors of α3β4 nAChRs. As suggested by molecular modeling techniques the novel derivatives explore additional space of interactions within the luminal domain of the studied nAChR subtype; the pattern of interactions should be selective for nAChRs containing the β4 subunit. Behavioral experiments are therefore consistent with involvement of the α3β4 nAChR in the pathomechanism of addiction and demonstrated that inhibition of α3β4 nAChR by N-alkylated DM derivatives is a promising approach in the treatment of addiction.

References and notes

1. Arias, H. R. Ligand-Gated Ion Channel Receptor Superfamilies. In _Biological and Biophysical Aspects of Ligand-Gated Ion Channel Receptor Superfamilies_; Arias, H. R., Ed.; Research Signpost: Kerala, India, 2006; pp 1–25.
2. Millar, N. S.; Gotti, C. _Neuropharmacology_ **2009**, _56_, 237.
3. Arias, H. R. _Adv. Protein Chem. Struct. Biol._ **2010**, _80_, 153.
4. Arias, H. R. _Brain Res. Rev._ **1997**, _25_, 133.
5. Arias, H. R. _Biochim. Biophys. Acta BBA—Rev. Biomembr._ **1998**, _1376_, 173.
6. Jozwiak, K.; Ravichandran, S.; Collins, J. R.; Wainer, I. W. _J. Med. Chem._ **2004**, _47_, 4008.
7. Glick, S. D.; Sell, E. M.; Maisonneuve, I. M. _Eur. J. Pharmacol._ **2008**, _599_, 91.
8. Gotti, C.; Zoli, M.; Clementi, F. _Trends Pharmacol. Sci._ **2006**, _27_, 482.
9. Toll, L.; Zaveri, N. T.; Polgar, W. E.; Jiang, F.; Khroyan, T. V.; Zhou, W.; Xie, X. S.; Stauber, G. B.; Costello, M. R.; Leslie, F. M. _Neuropsychopharmacology_ **2012**, _37_, 1367.
10. Glick, S. D.; Maisonneuve, I. M.; Kitchen, B. A.; Fleck, M. W. _Eur. J. Pharmacol._ **2002**, _438_, 99.
11. Salas, R.; Sturm, R.; Boulter, J.; Biasi, M. D. _J. Neurosci._ **2009**, _29_, 3014.
12. Salas, R.; Pieri, F.; Biasi, M. D. _J. Neurosci._ **2004**, _24_, 10035.
13. Taraschenko, O. D.; Panchal, V.; Maisonneuve, I. M.; Glick, S. D. _Eur. J. Pharmacol._ **2005**, _513_, 207.
14. Glick, S. D.; Maisonneuve, I. M.; Dickinson, H. A.; Kitchen, B. A. _Eur. J. Pharmacol._ **2001**, _422_, 87.
15. Ebert, B.; Thorkildsen, C.; Andersen, S.; Christrup, L. L.; Hjeds, H. _Biochem. Pharmacol._ **1998**, _56_, 553.
16. Hernandez, S. C.; Bertolino, M.; Xiao, Y.; Pringle, K. E.; Caruso, F. S.; Kellar, K. J. _J. Pharmacol. Exp. Ther._ **2000**, _293_, 962.
17. Jozwiak, K.; Moaddel, R.; Yamaguchi, R.; Ravichandran, S.; Collins, J. R.; Wainer, I. W. _J. Chromatogr. B., Analyt. Technol. Biomed. Life Sci._ **2005**, _819_, 169.
18. Jozwiak, K.; Hernandez, S. C.; Kellar, K. J.; Wainer, I. W. _J. Chromatogr. B., Analyt. Technol. Biomed. Life Sci._ **2003**, _797_, 373.
19. Xiao, Y.; Meyer, E. L.; Thompson, J. M.; Surin, A.; Wroblewski, J.; Kellar, K. J. _Mol. Pharmacol._ **1998**, _54_, 322.
20. Gasteiger, E.; Gattiker, A.; Hoogland, C.; Ivanyi, I.; Appel, R. D.; Bairoch, A. _Nucleic Acids Res._ **2003**, _31_, 3784.
21. Thompson, J. D.; Higgins, D. G.; Gibson, T. J. _Nucleic Acids Res._ **1994**, _22_, 4673.
22. Eswar, N.; Webb, B.; Marti-Renom, M. A.; Madhusudhan, M. S.; Eramian, D.; Shen, M.-Y.; Pieper, U.; Sali, A. _Curr. Protoc. Bioinformatics_ **2006**, _5_, 5.
23. Melo, F.; Feytmans, E. _J. Mol. Biol._ **1998**, _277_, 1141.
24. Bowie, J. U.; Luthy, R.; Eisenberg, D. _Science_ **1991**, _253_, 164.
25. Laskowski, R. A.; MacArthur, M. W.; Moss, D. S.; Thornton, J. M. _J. Appl. Crystallogr._ **1993**, _26_, 283.
26. LigPrep, Version 2.4: Schrödinger, LLC, New York, 2010.
27. Epik, Version 2.1: Schrödinger, LLC, New York, 2010.
28. Bowers, K. J.; Chow, E.; Xu, H.; Dror, R. O.; Eastwood, M. P.; Gregersen, B. A.; Klepeis, J. L.; Kolossváry, I.; Moraes, M. A.; Sacerdoti, F. D.; Salmon, J. K.; Shan, Y.; Shaw, D. E. Proceedings of the ACM/IEEE Conference on Supercomputing (SC06), Tampa, Florida, November 11–17, 2006.
29. Krieger, E.; Vriend, G. _Bioinformatics_ **2002**, _18_, 315.
30. The PyMOL Molecular Graphics System, Version 1.5.0.3, Schrödinger LLC.
31. Huang, E. Y.-K.; Liu, T.-C.; Tao, P.-L. _Naunyn-Schmiedeberg's Arch. Pharmacol._ **2003**, _368_, 386.
32. Biala, G.; Budzynska, B.; Staniak, N. _Behav. Brain Res._ **2009**, _202_, 260.
33. Biala, G.; Staniak, N. _Pharmacol. Biochem. Behav._ **2010**, _96_, 141.
34. Gosselin, G. E.; Roger, P. S.; Harold, C. H. _Clinical Toxicology of Commercial Products_, 5th Ed; Williams and Wilkins: Baltimore, MD, 1981.
35. Benson, W. M.; Stefko, P. L.; Randall, L. O. _J. Pharmacol. Exp. Ther._ **1953**, _109_, 189.
36. Santamaria, J.; Kaddachi, M. T.; Rigaudy, J. _Tetrahedron Lett._ **1990**, _31_, 4735.
37. Ferroud, C.; Rool, P.; Santamaria, J. _Tetrahedron Lett._ **1998**, _39_, 9423.
38. Craviso, G. L.; Musacchio, J. M. _Mol. Pharmacol._ **1983**, _23_, 629.
39. Wainer. I. W.; Jozwiak, K; Moaddel, R.; Ravichandran, S.; Collins, J. R. Patent US7749984.
40. Peet, N. P. _J. Pharm. Sci._ **1980**, _69_, 1447.
41. Targowska-Duda, K. M.; Arias, H. R.; Jozwiak, K. _Open Conf. Proc. J._ **2013**, _4_, 11.
42. Tzschentke, T. M. _Prog. Neurobiol._ **1998**, _56_, 613.